ISSN 1028-334X, Doklady Earth Sciences, 2023, Vol. 513, Suppl. 1, pp. S121–S139. © Pleiades Publishing, Ltd., 2023.

PALEOBOTANICS

Chronology and Main Stages of the Vegetation Development During the Mikulino Interglacial on the Russian Plain According to the Results of Buried Lake and Peat Sediments Study from Tver and Smolensk Province

F. E. Maksimov[a,*], L. A. Savelieva[a], A. P. Fomenko[b], S. S. Popova[c], I. S. Zyuganova[d], V.A. Grigoriev[a], A. Yu. Petrov[a], S. F. Boltramovich[a], and V. Yu. Kuznetsov[a,e]

Received September 10, 2023; revised September 21, 2023; accepted September 22, 2023

Abstract—The chronology of the Mikulino Interglacial and its individual phases has been the subject of discussion. The goal of this study is to evaluate the time limits of the main stages of the Mikulino Interglacial on the Russian Plain according to ^{230}Th/U dating and paleobotanical studies of lake and peat sediments from the known sections located in Tver Province on the Bolshaya Dubenka River, Malaya Kosha River, Granichnaya River, and Sizhina River (Kileshino-2 section). An improved geochronological approach has been applied to identify the layers that are suitable for the ^{230}Th/U isochronous approximation. Together with palynological and carpological studies, this made it possible to date the layers corresponding to relatively narrow time intervals in the development of plant formations at the different stages of the Last Interglacial. New paleobotanical studies of buried lake and peat sediments from the sections located on the Bolshaya Dubenka River, Malaya Kosha River, and Granichnaya River allowed us to reconstruct the vegetation development of the Mikulino Interglacial in the interval of pollen zones M1–M7, i.e., more pollen zones have been analyzed and in greater detail than in the 1960s–1970s. A chronological scheme of the main stages of the development of vegetation in the Mikulino Interglacial is proposed based on the results of ^{230}Th/U dating and paleobotanical studies of the deposits from the sections in Tver Province together with previously published data obtained for the Nizhnyaya Boyarshchina section in Smolensk Province. The beginning of the Mikulino Interglacial is recorded at about 130–126 ka. Its first phase, corresponding to the M2 zone, ended about 118 ka. The preoptimal stages of vegetation development (zones M3 and M4) fit into the time interval of about 118–112 ka, while the climatic optimum of the Interglacial (zones M5 and M6) began about 112 ka and ended about 100 ka. Thus, the duration of the Mikulino Interglacial was likely to be at least 25000 years.

Keywords: lake and peat sediments, East European Plain, geochronology, Mikulino Interglacial, MIS 5e, ^{230}Th/U dating method, isochronous approximation, palynological and carpological analyses

DOI: 10.1134/S1028334X23602481

INTRODUCTION

The Late Pleistocene on the Russian Plain has been under close attention for many decades and has been studied in an enormous number of scientific investigations. Nevertheless, there are still numerous questions that need comprehensive answers. For instance, the temporal parameters of this period continue to be the subject of discussion. A widespread view is based on the correlation between the Mikulino (Eemian) Interglacial and the marine isotope oxygen substage MIS-5e [1]. However, there are studies that suggest a longer duration of this period until the coverage of the entire MIS-5 stage [2].

In the paleogeographic reconstructions, the temporal boundaries of the Mikulino Interglacial are mostly established indirectly, i.e., taking into account the correlation with the oxygen-isotope curves. Quantitative dating of the Mikulino deposits is used primarily for comparing the dates with the MIS-5e substage. Deviations from MIS-5e are often considered as errors in the dating methods in use. Estimation of the

[a] *St. Petersburg State University, St. Petersburg, 199034 Russia*

[b] *Karpinsky Russian Geological Research Institute, St. Petersburg, 199106 Russia*

[c] *Komarov Botanical Institute, Russian Academy of Sciences, St. Petersburg, 197376 Russia*

[d] *Institute of Geography, Russian Academy of Sciences, Moscow, 119017 Russia*

[e] *Herzen State Pedagogical University of Russia, St. Petersburg, 191186 Russia*

**e-mail: maksimov-fedor@yandex.ru*

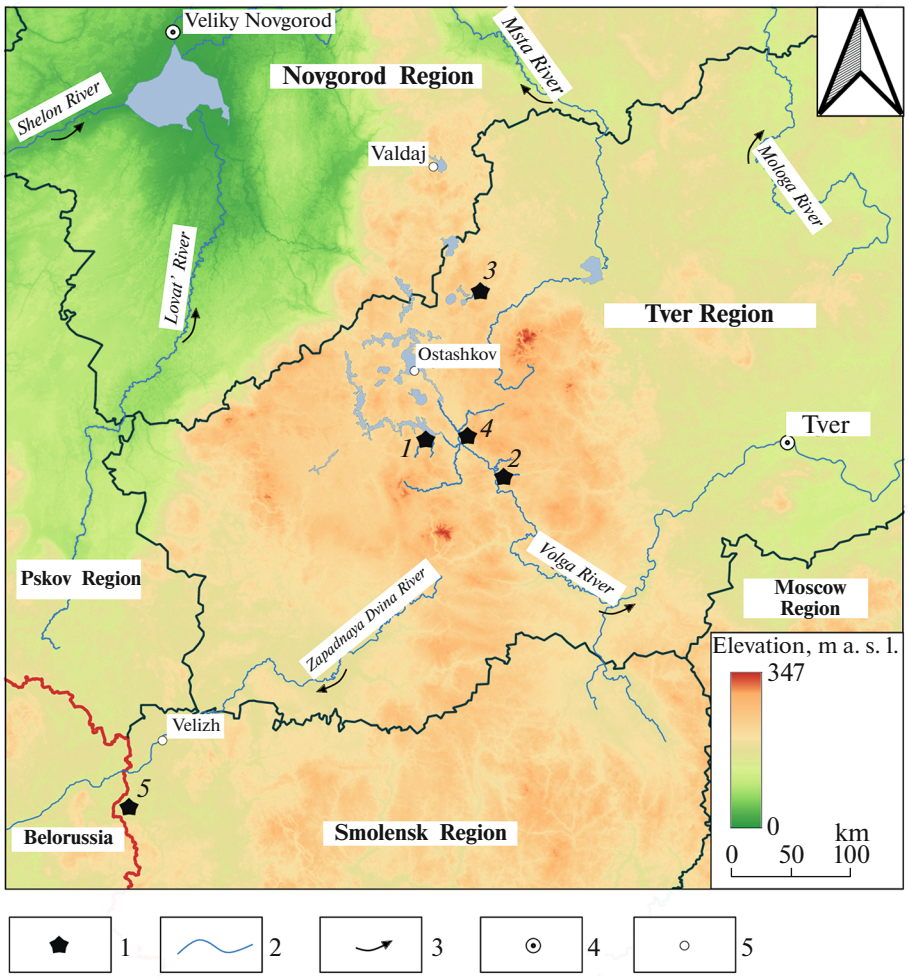

Fig. 1. Location of the studied sections. 1, Section ((*1*) Bolshaya Dubenka, (*2*) Malaya Kosha, (*3*) Granichnaya, (*4*) Kileshino-2, (*5*) Nizhnyaya Boyarshchina); 2, hydrological network; 3, direction of the river flow; 4, administrative center; 5, settlement.

chronology of the Mikulino horizon based directly on dating its deposits is rarely employed [3, 4].

We note that direct estimation of the Mikulino Interglacial chronology can be made when the sediments where its main phases are clearly identified can be dated. Such circumstances are combined in buried organic-rich sediments. The Mikulino Interglacial is clearly recognized in lake–peat and oxbow sediments. These are the sediments where a sequence of M1–M8 pollen zones has been identified, which allows us to track the characteristic vegetation changes on the Russian Plain specific only to the Last Interglacial [5]. On the other hand, the age of these deposits can be determined by the ^{230}Th/U method. Consequently, an approach based on paleobotanical studies and ^{230}Th/U dating of such sediments can be used effectively to construct a chronological scheme for the Mikulino Interglacial.

In several sections on the Russian Plain, we dated Mikulino organic-rich sediments to determine their chronostratigraphic position ([6] and others). As a rule, the ^{230}Th/U data reflected the age of the organic-rich stratum as a whole, i.e., several pollen zones, and could not be used for detailed chronology. Later on, our task was to distinguish individual phases of the development of vegetation and to perform their ^{230}Th/U dating in order to enhance the chronology of the Mikulino interglacial on the Russian Plain. From this perspective, this work examines new results of paleobotanical and geochronometric research on several sections known previously in Tver Province (Fig. 1) together with the published data on the Nizhnyaya Boyarshchina section [4]. Furthermore, we focus on the characteristic features of the Mikulino plant communities identified in these sections.

STUDY OBJECTS

Bolshaya Dubenka section. Outcrop Provinceon the right bank of the Bolshaya Dubenka River near the village of Sosnovatka (Tver Province) that expose the bedrock slope of the river valley, with a height from 5

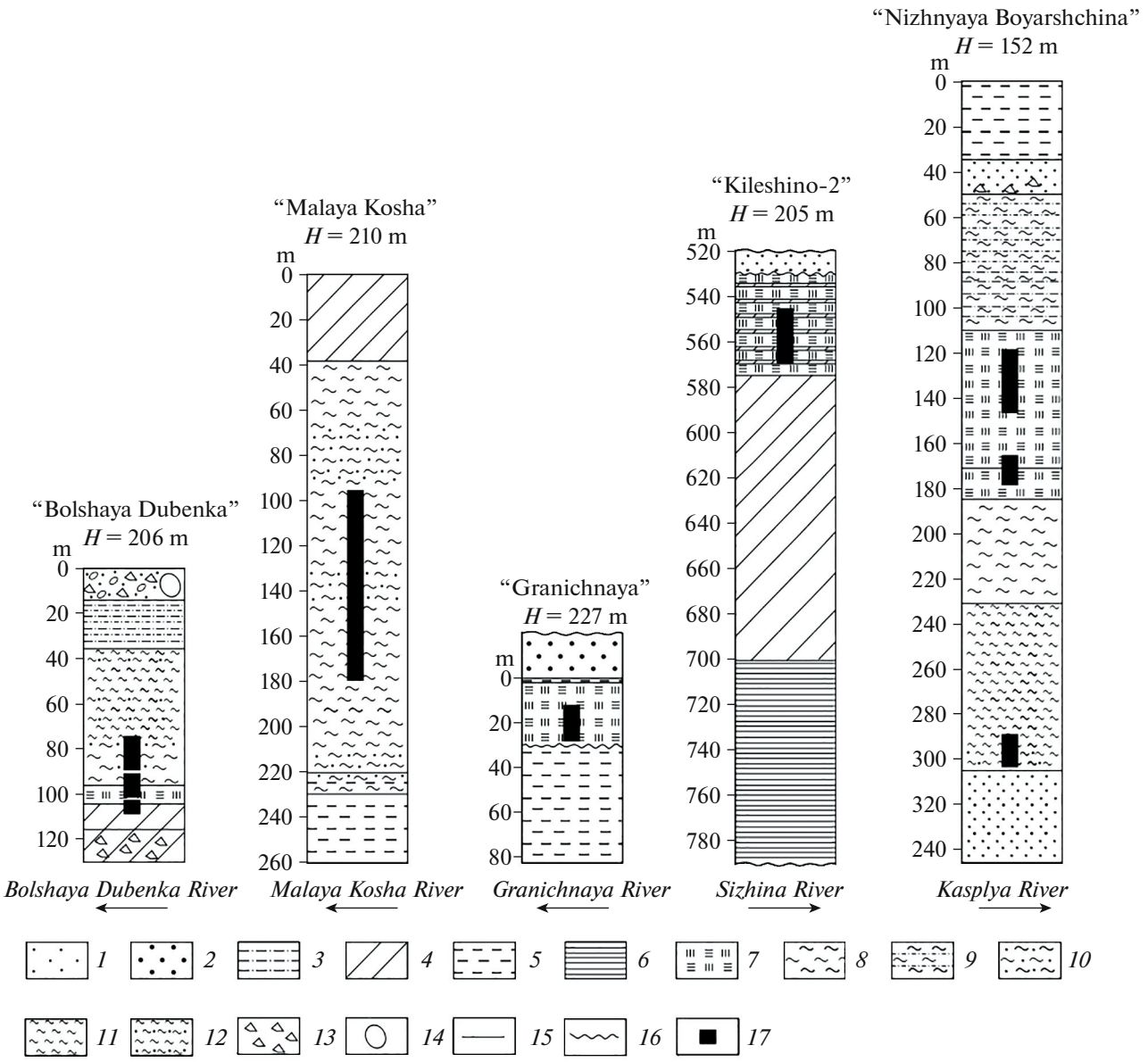

Fig. 2. Lithological cores of the Bolshaya Dubenka, Malaya Kosha, Granichnaya, Kileshino-2 [13], and Nizhnyaya Boyarshchina [4]) sections. (*1*) Fine-grained sand, (*2*) coarse sand, (*3*) silts, (*4*) loam, (*5*) clay, (*6*) rhythmically layered heavy loam, (*7*) peat, (*8*) gyttja, (*9*) silty gyttja, (*10*) sandy gyttja, (*11*) dense gyttja, (*12*) dense sandy gyttja, (*13*) gravel, (*14*) boulder, (*15*) boundaries between layers, (*16*) stratigraphic unconformity, (*17*) ^{230}Th/U age.

to 10 m above the edge of the water on a segment >350 m, were studied in the 1960s–1970s [7, 8]. The lake–peat sediments, ~2 m thick on average, overlying the surface of the Moscow moraine and covered by Valdai moraine formations and Holocene sediments were found to include the Mikulino Interglacial zones, first M4–M7 and later M3–M7.

In September 2020, organomineral sediments with a thickness slightly exceeding 1 m were exposed in the lower part of the bedrock slope of the river valley on the right bank of the Bolshaya Dubenka River (coordinates 56°52.511′ N, 33°11.289′ E, elevation 206 m) during the fieldwork (Fig. 2). The base of the exposed sediments was located 33 cm above the edge of the water, while their top (0 cm) was approximately 5 m below the crest.

The overall structure of the section closely resembles what was observed 50–60 years ago [7, 8]. The lake–peat sequence is confined between moraine deposits, as was previously established.

Malaya Koshas Section. This outcrop on the right bedrock bank of the Malaya Kosha River, ~1–1.5 km southwestern part of the village of Loshakovo (Tver Province), has long been known and of increased interest to researchers [7–9]. The sequence of

Mikulino lake–peat sediments is exposed over a length of about 80 m in the upper part of the bedrock slope of the river valley, with a height of 15–17 m above the edge of the water. A sequence 3- to 5-m thick overlies the Moscow-aged lacustrine–glacial clays and is covered by a "periglacial formation in the fluvial–glacial, deluvial–solifluction, and flood–glacial sediments formed during the Valdai glaciation" [9] with an average thickness of 4.0–4.5 m.

In September 2021, we collected samples from an outcrop located on the right bank of the Malaya Kosha River (coordinates 56°43.460′ N, 33°44.484′ E, elevation 210 m) in the upper outcropped portion of the bedrock slope. It exposed the gyttja layers covered by clay loams and underlain by gray–blue clays 4.6 m below the crest of the slope (Fig. 2). At the depth of 185–190 cm from the top of the section (0 cm), there is a confining overlying bed below which everything is waterlogged. Above 0 cm there are brown clays; the contact with clay loams is sharp.

The total height of the upper outcropped portion of the bedrock slope on the right bank of the river is ~7–8 m. The lower portion of the slope is covered by landslides. From the bottom of the outcropped sediments to the edge of the water is ~8–9 m. The right bank is described almost the same way by E.N. Ananova et al. [8].

The structure of the section differs slightly from the data published earlier [7–9]. This can be related to rejuvenation of the section in the past 50–60 years, as well as to sections drifted on various location points of the lens of lake and peat sediments, having gyttjas as the main layer in all cases, including our case.

Granichnaya section. The Mikulino sediments on the Granichnaya River near the village of Novoe Koz'yanovo (Tver Province) are located in the marginal zone of the Valdai glaciation [10]. On top they are covered by a thin Valdai moraine and are underlain by deposits of the Kasplya Interstadial of the Moscow Interglacial; beneath lies the Moscow moraine.

In September 2021, we made a pit on the right concave bank at the meander of the Granichnaya River in the bedrock slope of the river valley (coordinates 57°28.699′ N, 33°35.359′ E, elevation 227 m). It exposed layers of sand, peat, and gray–blue clays top to bottom (Fig. 2). There is a distinct and uneven boundary between the peat and the underlying clays, which may indicate a sedimentary hiatus. The vertical profile of the exposed deposits, from their lowest point (80 cm) to the edge of the water, is ~70 cm, while from their top (0 cm) to the edge of the riverbank (the surface of the first floodplain terrace) it is 200–250 cm. Therefore, the height of the riverbank, ~4 m, corresponds to the description by I.V. Kotlukova [10]. However, the structure of the section is somewhat different. In our case, the peat layer is sandwiched between sands above and clays below, while in 1972, it was the opposite—clays above and sands below. Evidently, in the span of 50 years, the situation has changed, and coastal erosion has exposed the significant variability in the Quaternary section at this location.

For each of the sections described, we collected samples from organic-rich deposits and host sediments at intervals of 1–4 cm for paleobotanical analysis, loss on ignition (LOI) calculation, and ^{230}Th/U dating.

Furthermore, we considered the well-known section on the eastern outskirts of the village of Kileshino (Kileshino-2), confined to the left undercut slope of the Sizhina River valley in Tver Province [7, 11]. The stratigraphic position of the lower organic-rich layer was unclear; it was referred to both the Mikulino time [11] and the middle Valdai Interstadial [12].

In 2018, researchers from the Institute of Geography, Russian Academy of Sciences (IG RAS), cleared the Kileshino-2 outcrop (coordinates 56°52.8264′ N, 33°27.4980′ E, elevation 210 m) on the left bank of the Sizhina River at the top of the meander and collected samples for paleobotanical analysis and radiocarbon dating [13]. In the same year (two weeks later than our IG RAS colleagues did), we collected samples on the interval of 2–5 cm from the lower organogenic layer for ^{230}Th/U dating on the same exposure.

METHODS OF STUDY

Uranium–Thorium Method

To establish the time intervals for certain stages in the Mikulino Interglacial, we used the ^{230}Th/U method, which makes it possible to date organic-rich deposits with ages up to 300–350 ka [4]. These formations consist of organic and mineral components; therefore, to determine their ^{230}Th/U age, we need to make a correction for the initial (incorporated into the deposits at the time of their formation) isotopic contamination. To do this, we use an isochronous approximation, which is based on quantification of the U and Th isotopes in a series of same-age samples ([6, 14], and others). The conditions for its application were characterized in detail in [4]. In brief, they can be summarized as follows. At the time of deposit formation, the organic component accumulates hydrogenous uranium that produces ^{230}Th with time. This fraction is datable. The values of the activity ratios in the mineral (detrital) fraction, ^{230}Th/^{234}U, ^{234}U/^{238}U, ^{230}Th/^{232}Th, remain constant from sample to sample, i.e., indicating a single source of primary thorium contamination. Finally, the deposits as a whole should belong to a closed radiometric system relative to the U and Th isotopes during the post-sedimentation time.

Consequently, we can construct the linear dependences and determine the values of the ^{230}Th/^{234}U and ^{234}U/^{238}U activity ratios in the datable organic fraction in the coordinates of ^{230}Th/^{232}Th–^{234}U/^{232}Th and

$^{234}U/^{232}Th$–$^{238}U/^{232}Th$ for a series of same-age samples to use them in isochronous age calculations.

The specific activities of the U and Th isotopes in the samples collected along the vertical profile of the deposits were determined taking into account their complete dissolution (a TSD model) using a radiochemical technique [6, 15]. Simultaneously, we calculated the losses on ignition (LOI). The samples of the same age suitable for isochronous dating were selected based on several conditions.

First, we tested if the samples belonged to a closed radiometric system. At the preliminary stage, we determined the value of the $^{228}Th/^{232}Th$ activity ratio in the samples. If its value deviated from unity by more than $\pm 1\sigma$ (σ is the measurement error), this indicated a violation of the radioactive equilibrium in the chain of three genetically related isotopes, $^{232}Th \rightarrow {}^{228}Ra \rightarrow {}^{228}Th$, at some instant during the past 25–30 years. It is not unlikely that, in this case, the thorium isotopes ^{228}Th, ^{232}Th, and ^{230}Th might have migrated, which resulted in violation of an important premise of the method. To avoid introducing this uncertainty, we did not further consider the samples with significant deviations of the value of the $^{228}Th/^{232}Th$ activity ratio from unity (by more than $\pm 1\sigma$).

Later on, we analyzed the distribution of the $^{230}Th/^{234}U$ and $^{234}U/^{238}U$ activity ratios and the U content in the samples along the vertical profile of the organic-rich sequence of sediments. Significant fluctuations in these values of individual samples could also indicate violations of the closed system conditions, mostly associated with the migration of water-soluble U forms in the post-sedimentation time. Accordingly, we excluded the samples attributed to open systems from the same-age series.

In isochronous diagrams, the points corresponding to the samples of open systems often deviate noticeably from the linear dependences. However, in some cases, this deviation is not so pronounced. Moreover, if samples have multiple sources of thorium contamination, this may result only in a slight deviation from the linear dependencies. Therefore, we additionally used the coordinates of $^{230}Th/^{234}U$–$^{232}Th/^{234}U$ and $^{234}U/^{238}U$–$^{232}Th/^{238}U$, where the mismatch of the points to the linear regression is more evident [4].

The reliability of isochronous structures depends to some extent on the range of point locations along the linear dependences. Therefore, when possible, we selected the segments of the vertical profile of the sediments with significant variations in the values of the $^{230}Th/^{232}Th$ activity ratios for dating.

To use the isochronous approximation correctly, we should take the samples of the same or close ages into account. Therefore, we used the vertical profile segments formed in rather narrow time intervals, for example, within one or, in extreme cases, several pollen zones.

The isochronous age was calculated using the analytical data from a series of samples of the same age by linear and nonlinear techniques [4]. In this case, the reliability of dating was higher than if only one of them was used. As a final estimation of the $^{230}Th/U$ isochronous age, we examined the time interval of overlap between the confidence intervals obtained by both linear and nonlinear techniques.

Pollen Analysis

To conduct the pollen analysis, we collected 28 samples on an interval of 2–8 cm from the section of the Bolshaya Dubenka River, 44 samples of the Malaya Kosha River, and 19 samples of the Granichnaya River. The microfossils were extracted from the deposits of the samples weighing 1–2 g by the standard procedure [16, 17].

Paleocarpological Analysis

In the section of the Malaya Kosha River, we collected samples with a volume of 500–600 cm^3 for the carpological analysis from the layers containing plant remains (peat and peaty clays). In the section of the Bolshaya Dubenka River, we analyzed a series of small volume samples that were selected for the pollen analysis. The plant remains were extracted by the standard procedure [18].

The detailed descriptions of the procedure for microfossil extraction from deposits, plotting of diagrams, deliniation of pollen zone boundaries, and the taxonomic identification of pollen and macroremains were provided in the work published earlier [4].

RESULTS OF THIS STUDY

The experimental data are presented separately for each section in the sequence: paleobotanical description of the vegetation zones, identification of the Mikulino Interglacial phases, and their $^{230}Th/U$ dating.

Bolshaya Dubenka Section

Pollen analysis. Nine palynozones were identified (Fig. 3).

Pollen zone 1 (126–116 cm). Among tree pollen, dominant are *Pinus* (27%) and *Betula sect. Albae* (14%). *Betula nana* pollen is recorded (9%). The contents of *Alnus* and *Corylus* pollen are 11% and 6%, respectively. Grass pollen accounts for about 30%. Among spore plants, *Polypodiaceae* spores are dominant. The content of pre-Quaternary spores and pollen reaches 80%.

Pollen zone 2 (116–110.5 cm). *Pinus* pollen predominates (47%). The content of *Picea* pollen increases (up to 13%). The count of Polypodiaceae

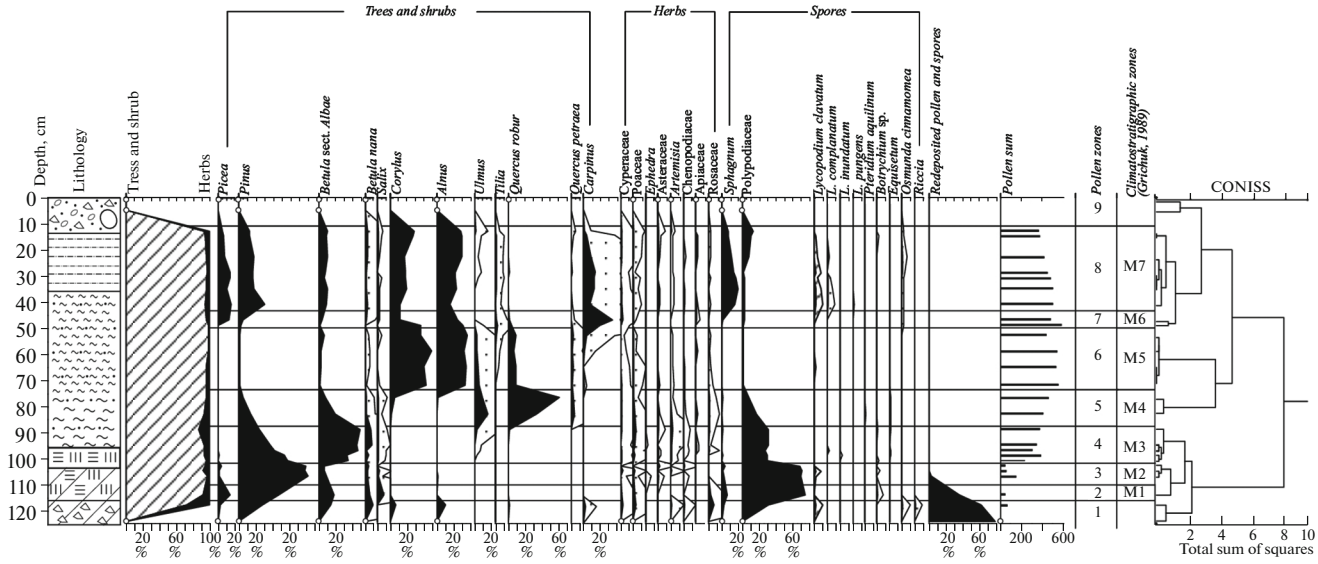

Fig. 3. Spore–pollen diagram of the Bolshaya Dubenka section.

spores rises (up to 70%). The content of pre-Quaternary spores and pollen decreases to 34%.

Pollen zone 3 (110.5–102 cm). *Picea* pollen gradually diminishes in the spectra. Herbaceous plants are represented by pollen from the families Cyperaceae, Poaceae, and Chenopodiaceae, as well as the genera *Ephedra* and *Artemisia*. The content of pre-Quaternary spores and pollen significantly decreases (down to 5%).

Pollen zone 4 (102–88 cm). *Betula* sect. *Albae* pollen prevails (33–48%). Pollen from broadleaved species, such as *Ulmus* and *Quercus robur,* is recorded for the first time. The count of Polypodiaceae spores decreases to 27%.

Pollen zone 5 (88–74 cm). This zone is characterized by a high content of *Quercus robur* (34–61%) and *Ulmus* pollen (up to 16%). The amount of *Quercus petraea* pollen is 2–5%. The content of Polypodiaceae spores decreases to 7%.

Pollen zone 6 (74–50 cm). *Alnus* (maximum 37%) and *Corylus* (maximum 49%) pollens dominate. The amount of *Quercus robur* pollen decreases to 10%. *Carpinus* pollen is recorded (up to 4%). *Tilia* pollen grains are identified.

Pollen zone 7 (50–43 cm). *Carpinus* pollen reaches its maximum (34%), along with *Tilia* (2%). *Quercus robur* and *Quercus petraea* pollens are present in minute amounts. Spores of *Osmunda cinnamomea* are encountered for the first time.

Pollen zone 8 (43–9 cm): A maximum of *Picea* pollen is observed (up to 16%). Among thermophilic tree and shrub species, *Corylus* (up to 29%) and *Carpinus* (up to 14%) pollens dominate. The proportion of *Sphagnum* (8–19%) and *Polypodiaceae* spores (up to 13%) increases. Spores of *Osmunda cinnamomea* are recorded.

Pollen zone 9 (9–0 cm): Pollen grains of *Picea, Pinus, Betula* sect. *Albae, Betula nana*, *Alnus,* and *Quercus robur* occur sporadically.

The comparison of the data obtained with the results of the previous studies of deposits on the Bolshaya Dubenka River [7, 8] revealed the similarities in the spore and pollen spectra with the stages of vegetation development during the Mikulino Interglacial (M1–M7 zones).

On the surface of the glacial deposit (M1 zone), pioneer vegetation was widespread; spruce might have been present. At the early stage of the Mikulino Interglacial (M2 zone), taiga forests played a minor role, but spruce was found in such forests. Ferns and miscellaneous herbs were abundant. Later on (M3 zone), broadleaved species began to encroach on the territory. The role of birch–pine tree forests increased. Abundant and diverse species were recorded in the grass layer. Lacustrine sedimentation began. During the time corresponding to the M4 zone, forests in which oak and elm trees were dominants became widespread. Broadleaved forests, represented mainly by linden (M5 zone) and hornbeam (M6 zone), successively developed during the Mikulino Interglacial optimum. Hazel grew in the shrub layer. Heat-loving ferns, e.g., Osmunda, appeared at the end of the optimum. Later on (M7 zone), birch–pine tree forests were widespread, with an increased proportion of moisture-loving spruce.

Paleocarpological analysis. Carpological remains are detected in the interval of 86–108 cm. The samples from the upper portion of the aleurite layer (depth of 104–108 cm) were found to contain only single fruits

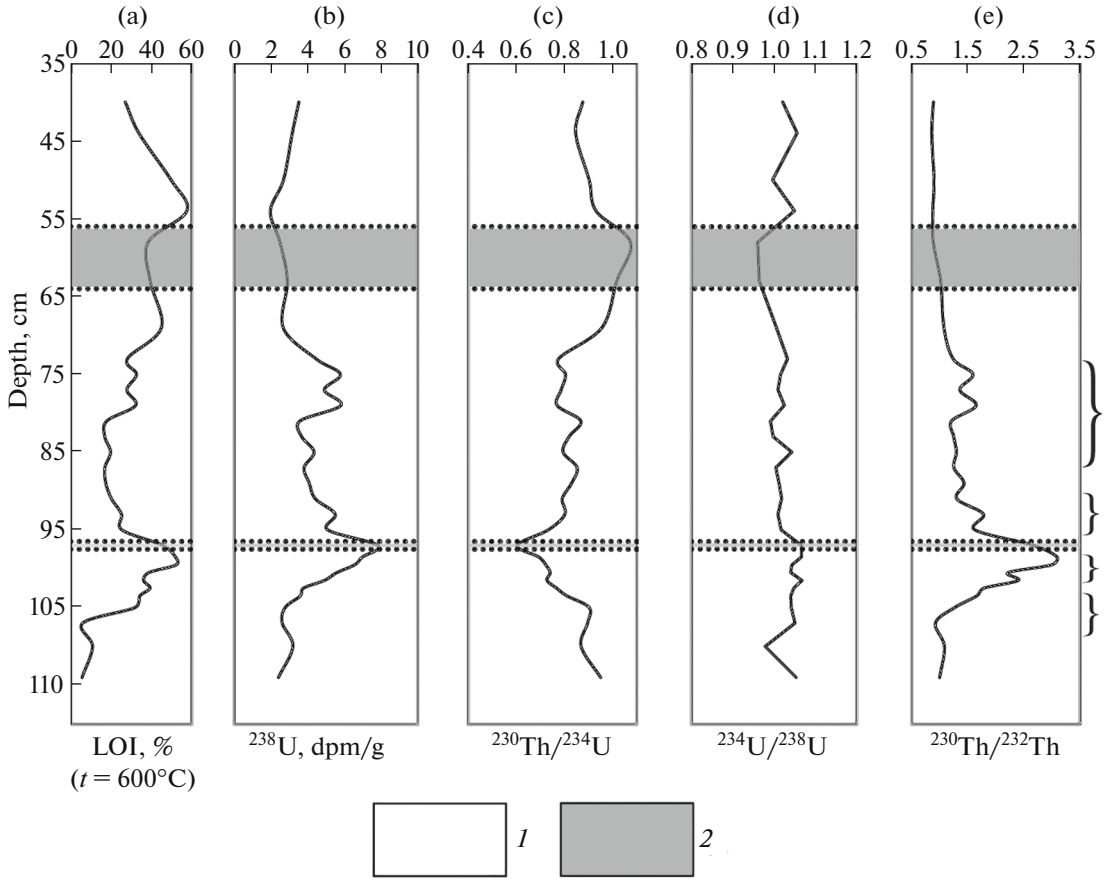

Fig. 4. Distribution of organic matter (LOI, loss on ignition), U, and ratios of $^{230}Th/^{234}U$, $^{234}U/^{238}U$, and $^{230}Th/^{232}Th$ activities along the vertical profile of the lake and peat sequence of the Bolshaya Dubenka section. The curly brackets show the sites selected for $^{230}Th/U$ isochronous dating. (*1*) Closed radiometric system; (*2*) geochemical barrier (open radiometric system).

and seeds of marsh plants (*Carex* sp., *Comarum palustre*). In the peat layer (depth of 96–104 cm), remains of woody plants were identified, including numerous birch nutlets and scales (*Betula* sect. *Betula*), as well as single alder nutlets (*Alnus* cf. *glutinosa*) and the seeds of spruce (*Picea* sp.). In addition, remains of moderately thermophilic aquatic plants were identified, such as seeds of *Stratiotes aloides* and *Lemna trisulca*, as well as the fruits of *Ceratophyllum demersum*. Marsh and semiaquatic plants are represented by the remains of *Comarum palustre*, *Menyanthes trifoliata*, *Carex* sp., and *Scirpus* sp. In addition, isolated remains of meadow plants, including *Stachys annua*, *Fragaria vesca*, and *Potentilla reptans*, were recorded. The samples from the bottom layer of sandy gyttja (depth of 86–96 cm) were found to contain single birch nutlets, as well as fruits of *Ceratophyllum demersum* and some marsh plants.

The comparison of the paleocarpological and palynological data (Fig. 3) revealed that the local carpological complexes (LCCs) of Bolshaya Dubenka section belong to the upper portion of M2 palynological zone, M3, and the beginning of M4 zone, i.e., to the early stage of the Mikulino Interglacial.

$^{230}Th/U$ dating. U and Th isotopes were determined in the samples of gyttja and peat along the vertical profile in the depth range of 38–116 cm. The values of the $^{228}Th/^{232}Th$ activity ratio in the samples did not deviate from unity by more than $\pm 1\sigma$ (σ is the measurement error), i.e., radioactive equilibrium between these isotopes was maintained over the last 25–30 years. The plot of the distribution of the $^{230}Th/^{234}U$, $^{234}U/^{238}U$, and U content along the vertical profile of the organic-rich stratum of the deposits showed the geochemical barriers, which are open radiometric systems during the post-sedimentation time (Fig. 4).

The upper barrier (56–64 cm) is likely associated with post-sedimentation preferential leaching of ^{234}U upon contact with the surrounding water according to the Cherdyntsev-Chalov effect [19]. This is indicated by both the values of $^{234}U/^{238}U$, which are lower than the equilibrium value that is equal to 1, and the values of the $^{230}Th/^{234}U$ activity ratios in these samples, which are ≥ 1.

The lower barrier is quite narrow; one sample from a depth of 96–98 cm showed significantly low values of the $^{230}Th/^{234}U$ activity ratios and at the same time

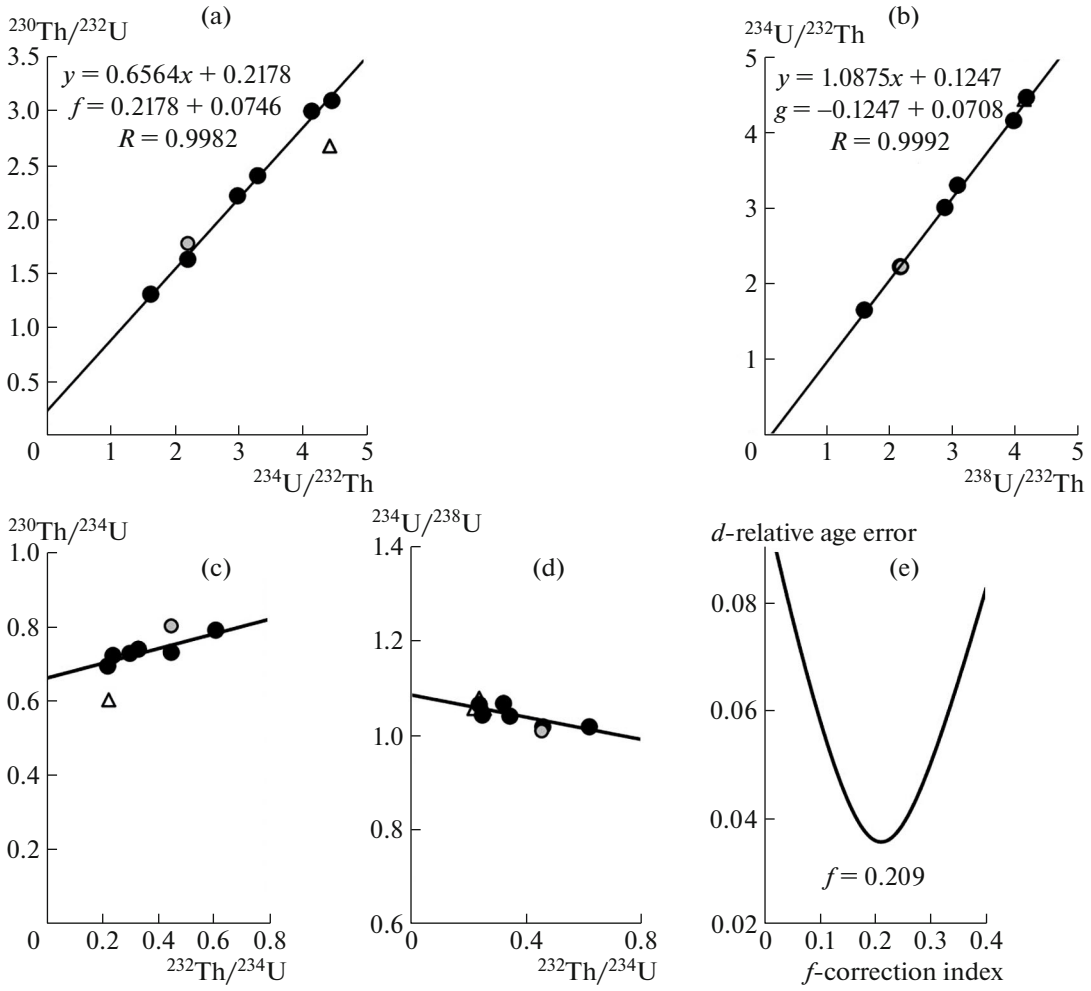

Fig. 5. Graphical representation of isochronous age determination by two calculation techniques for organic-rich deposits from the Bolshaya Dubenka section. (a), (b), (c), (d) Linear dependences plotted for six peat samples from the depth of 90–102 cm; (f), (g) values of correction indices, which are used to calculate the isochronous age of six samples from the depth of 90–102 cm by a linear technique. ● samples for which linear dependencies are constructed; ⊙ sample from the depth of 92–94 cm deviating from linearity; Δ sample from the depth of 96–98 cm assigned to an open radiometric system; (e) finding the f value required to calculate the isochronous age of six samples from the depth of 90–102 cm by a nonlinear technique.

somewhat elevated uranium content. Here, conversely, we recorded post-sedimentation accumulation by the deposits of water-soluble U forms from the surrounding waters.

We assume that the deposits outside these barriers could belong to closed radiometric systems during the post-sedimentation time.

Taking into account the above, we applied the isochronous approximation of the $^{230}Th/U$ method for the analytical data from three sets of samples within the depth intervals along the vertical profile: 74–90, 90–102, and 102–108 cm (Table 1), corresponding to the M4, M3, and M2 pollen zones.

Figure 5 shows a graphical representation for two methods of calculating the isochronous age on the interval of 90–102 cm (Fig. 5). The sample from the depth of 96–98 cm that belongs to the open radiometric system evidently deviates from the linear dependences in the coordinates of $^{230}Th/^{232}Th$–$^{234}U/^{232}Th$ and $^{230}Th/^{234}U$–$^{232}Th/^{234}U$. Another sample does not entirely conform to linearity, probably due to the presence of several sources of primary thorium contamination, and is therefore also excluded from consideration.

Table 2 provides the results of isochronous dating of the deposits for three segments at the depth intervals of 74–90, 90–102, and 102–108 cm and shows their correspondence to the pollen zones of the Mikulino Interglacial.

Malaya Kosha Section

Pollen analysis. Seven pollen zones were identified (Fig. 6).

Table 1. Results of radiochemical analysis of uranium and thorium isotopes in the samples of organogenic deposits from the studied sections in Tver Province

Depth, cm	LOI %	^{238}U	^{234}U	^{230}Th	^{232}Th	$\frac{^{230}Th}{^{234}U}$	$\frac{^{234}U}{^{238}U}$
		dpm/g					
Bolshaya Dubenka Section					Depth interval of 74–90 cm		
74–76	32.7	5.7742 ± 0.1697	5.8671 ± 0.1719	4.7139 ± 0.1476	2.9685 ± 0.1025	0.8035 ± 0.0345	1.0161 ± 0.0291
76–78	27.9	4.8985 ± 0.0954	4.9424 ± 0.0962	3.8806 ± 0.0846	2.8642 ± 0.0662	0.7852 ± 0.0229	1.0090 ± 0.0182
78–80	32.2	5.8025 ± 0.1510	5.9462 ± 0.1541	4.5692 ± 0.1281	2.7756 ± 0.0852	0.7684 ± 0.0293	1.0248 ± 0.0240
80–82*	17.9	3.5697 ± 0.0718	3.5390 ± 0.0714	3.0672 ± 0.0779	2.5382 ± 0.0673	0.8667 ± 0.0281	0.9914 ± 0.0205
82–84	16.9	3.6571 ± 0.0734	3.6476 ± 0.0733	2.9856 ± 0.0745	2.3982 ± 0.0633	0.8185 ± 0.0262	0.9974 ± 0.0205
84–86*	19.8	4.3402 ± 0.0998	4.5260 ± 0.1030	3.5896 ± 0.0845	2.7757 ± 0.0691	0.7931 ± 0.0260	1.0428 ± 0.0239
86–88	16.9	3.7958 ± 0.0832	3.8093 ± 0.0835	3.2435 ± 0.0784	2.5975 ± 0.0662	0.8515 ± 0.0278	1.0036 ± 0.0228
88–90	17.4	4.0772 ± 0.0795	4.1255 ± 0.0803	3.4179 ± 0.0840	2.3920 ± 0.0640	0.8285 ± 0.0260	1.0118 ± 0.0195
					Depth interval of 90–102 cm		
90–92	20.2	4.4014 ± 0.1028	4.4830 ± 0.1044	3.5413 ± 0.1027	2.7256 ± 0.0836	0.7899 ± 0.0294	1.0185 ± 0.0238
92–94*	25.2	5.4932 ± 0.1178	5.5457 ± 0.1188	4.4403 ± 0.1017	2.5004 ± 0.0648	0.8007 ± 0.0251	1.0096 ± 0.0202
94–96	25.4	5.0757 ± 0.1139	5.1616 ± 0.1154	3.7785 ± 0.1038	2.3302 ± 0.0718	0.7320 ± 0.0259	1.0169 ± 0.0216
96–98*	45.7	7.8123 ± 0.1404	8.3272 ± 0.1484	5.0161 ± 0.1134	1.8810 ± 0.0509	0.6024 ± 0.0173	1.0659 ± 0.0139
98–99	52.0	6.9746 ± 0.1170	7.4313 ± 0.1236	5.1454 ± 0.1107	1.6672 ± 0.0436	0.6924 ± 0.0188	1.0655 ± 0.0126
99–100	52.4	6.5514 ± 0.1208	6.8268 ± 0.1251	4.9220 ± 0.1068	1.6448 ± 0.0435	0.7210 ± 0.0205	1.0420 ± 0.0143
100–101	38.8	5.5803 ± 0.0982	5.8044 ± 0.1014	4.2934 ± 0.0905	1.9376 ± 0.0481	0.7397 ± 0.0203	1.0402 ± 0.0151
101–102	36.1	4.9118 ± 0.1028	5.2438 ± 0.1083	3.8092 ± 0.0968	1.5890 ± 0.0502	0.7264 ± 0.0238	1.0676 ± 0.0202
					Depth interval of 102–108 cm		
102–103	39.4	3.7604 ± 0.0752	3.9405 ± 0.0780	3.0191 ± 0.0834	1.6912 ± 0.0539	0.7662 ± 0.0260	1.0479 ± 0.0198
103–104	34.3	3.5887 ± 0.0760	3.7306 ± 0.0783	3.0188 ± 0.0729	1.8214 ± 0.0495	0.8092 ± 0.0259	1.0395 ± 0.0217
104–106	31.9	2.7633 ± 0.0605	2.8773 ± 0.0626	2.5941 ± 0.0706	2.0514 ± 0.0591	0.9016 ± 0.0314	1.0413 ± 0.0235
106–108	6.0	2.6017 ± 0.0646	2.7329 ± 0.0669	2.4464 ± 0.0722	2.6585 ± 0.0765	0.8952 ± 0.0343	1.0504 ± 0.0294
Kileshino Section					Depth interval of 545–570 cm		
545–548	22.8	5.8893 ± 0.1154	5.9375 ± 0.1162	4.5902 ± 0.1227	2.3709 ± 0.0707	0.7731 ± 0.0256	1.0082 ± 0.0157
545–548	22.8	5.8474 ± 0.1144	5.9262 ± 0.1158	4.3688 ± 0.1011	2.2380 ± 0.0578	0.7372 ± 0.0223	1.0135 ± 0.0156
548–550	18.8	4.1310 ± 0.0747	4.2877 ± 0.0770	3.5498 ± 0.0848	2.3224 ± 0.0599	0.8279 ± 0.0248	1.0379 ± 0.0161
550–554	13.2	2.4687 ± 0.0508	2.4504 ± 0.0506	2.2532 ± 0.0652	2.2215 ± 0.0644	0.9195 ± 0.0327	0.9926 ± 0.0209
554–557	10.0	2.1970 ± 0.0469	2.1547 ± 0.0465	1.9690 ± 0.0407	2.1745 ± 0.0439	0.9138 ± 0.0273	0.9807 ± 0.0220
557–559	19.3	2.4562 ± 0.0444	2.4653 ± 0.0445	2.2188 ± 0.0520	2.0551 ± 0.0490	0.9000 ± 0.0266	1.0037 ± 0.0175
559–561	17.0	2.3708 ± 0.0446	2.3552 ± 0.0446	2.0824 ± 0.0476	2.0270 ± 0.0465	0.8842 ± 0.0262	0.9934 ± 0.0186
561–563	24.1	2.7359 ± 0.0573	2.7615 ± 0.0580	2.2906 ± 0.0557	1.8030 ± 0.0455	0.8295 ± 0.0266	1.0094 ± 0.0201
563–565	23.8	2.3943 ± 0.0448	2.4706 ± 0.0459	2.0412 ± 0.0480	1.4948 ± 0.0378	0.8262 ± 0.0248	1.0319 ± 0.0186
565–570	18.0	2.2800 ± 0.0478	2.3661 ± 0.0493	1.6278 ± 0.0406	0.3170 ± 0.0149	0.6880 ± 0.0224	1.0378 ± 0.0221
565–570	18.0	2.3363 ± 0.0442	2.5099 ± 0.0467	1.7478 ± 0.0336	0.3452 ± 0.0117	0.6964 ± 0.0186	1.0743 ± 0.0198
Malaya Kosha Section					Depth interval of 96–180 cm		
96–98	9.3	1.9750 ± 0.0515	1.9473 ± 0.0511	1.8782 ± 0.0648	2.4369 ± 0.0797	0.9645 ± 0.0418	0.9860 ± 0.0279
112–114	6.3	1.8817 ± 0.0556	1.9101 ± 0.0562	1.7409 ± 0.0568	2.3284 ± 0.0714	0.9114 ± 0.0400	1.0151 ± 0.0330
116–118	6.5	1.6925 ± 0.0498	1.7224 ± 0.0503	1.6838 ± 0.0595	2.2679 ± 0.0756	0.9776 ± 0.0448	1.0176 ± 0.0328
120–122	13.4	2.2166 ± 0.0479	2.1891 ± 0.0475	2.0923 ± 0.1023	2.8151 ± 0.1322	0.9558 ± 0.0511	0.9876 ± 0.0212
122–124*	15.2	2.3030 ± 0.0716	2.4106 ± 0.0740	2.1016 ± 0.0525	2.7822 ± 0.0665	0.8718 ± 0.0345	1.0467 ± 0.0329
124–126	9.7	1.7122 ± 0.0556	1.7101 ± 0.0556	1.5965 ± 0.0445	2.1189 ± 0.0557	0.9335 ± 0.0400	0.9988 ± 0.0361

Table 1. (Contd.)

Depth, cm	LOI %	^{238}U	^{234}U	^{230}Th	^{232}Th	$\frac{^{230}Th}{^{234}U}$	$\frac{^{234}U}{^{238}U}$
		dpm/g					
126–128*	13.3	2.2117 ± 0.0647	2.2472 ± 0.0654	1.9523 ± 0.0854	2.5443 ± 0.1063	0.8687 ± 0.0457	1.0161 ± 0.0311
128–130*	11.7	1.9832 ± 0.0525	1.9624 ± 0.0525	1.6713 ± 0.0587	2.1437 ± 0.0699	0.8517 ± 0.0376	0.9895 ± 0.0303
130–132	11.5	1.6586 ± 0.0574	1.7304 ± 0.0590	1.4939 ± 0.0452	1.8440 ± 0.0531	0.8633 ± 0.0393	1.0433 ± 0.0405
132–134*	12.4	1.5245 ± 0.0425	1.6205 ± 0.0444	1.3836 ± 0.0496	1.7704 ± 0.0584	0.8538 ± 0.0385	1.0630 ± 0.0348
166–168*	8.2	1.0397 ± 0.0323	1.0609 ± 0.0330	0.9805 ± 0.0315	1.0940 ± 0.0336	0.9242 ± 0.0413	1.0204 ± 0.0382
168–170*	10.3	1.4572 ± 0.0514	1.2768 ± 0.0473	1.1220 ± 0.0387	1.3327 ± 0.0434	0.8787 ± 0.0445	0.8762 ± 0.0374
170–172*	12.8	1.6033 ± 0.0874	1.4684 ± 0.0824	1.3640 ± 0.0460	1.4927 ± 0.0490	0.9289 ± 0.0608	0.9159 ± 0.0588
172–174*	8.9	1.0249 ± 0.0450	0.9829 ± 0.0449	0.8430 ± 0.0222	0.9654 ± 0.0244	0.8577 ± 0.0452	0.9590 ± 0.0519
174–176	16.4	1.7552 ± 0.0470	1.7466 ± 0.0470	1.5087 ± 0.0436	1.5154 ± 0.0438	0.8638 ± 0.0341	0.9951 ± 0.0288
176–178	14.7	1.5392 ± 0.0402	1.6423 ± 0.0423	1.3806 ± 0.0355	1.4394 ± 0.0367	0.8406 ± 0.0306	1.0670 ± 0.0298
178–180	13.0	1.3346 ± 0.0386	1.3521 ± 0.0389	1.1583 ± 0.0362	1.1557 ± 0.0361	0.8567 ± 0.0364	1.0131 ± 0.0334
		Granichnaya Section			Depth interval of 2–12 cm		
2–4	49.3	9.4952 ± 0.2657	9.4426 ± 0.2646	3.0359 ± 0.0864	2.7508 ± 0.0800	0.3215 ± 0.0128	0.9945 ± 0.0236
4–6	37.8	3.0682 ± 0.0996	2.9560 ± 0.0969	2.4403 ± 0.0755	2.7091 ± 0.0822	0.8255 ± 0.0372	0.9634 ± 0.0324
8–10	39.5	3.2911 ± 0.0722	3.1615 ± 0.0701	2.6298 ± 0.0941	2.8497 ± 0.1003	0.8318 ± 0.0350	0.9606 ± 0.0214
10–12	37.4	3.5946 ± 0.1077	3.6060 ± 0.1082	3.1920 ± 0.0997	3.3266 ± 0.1029	0.8852 ± 0.0383	1.0032 ± 0.0313
					Depth interval of 12–28 cm		
12–14	34.0	2.7726 ± 0.0898	2.8295 ± 0.0911	2.3017 ± 0.0847	2.4254 ± 0.0882	0.8135 ± 0.0398	1.0205 ± 0.0350
14–16	60.6	2.6320 ± 0.0561	2.5907 ± 0.0554	2.1687 ± 0.0605	2.1467 ± 0.0599	0.8371 ± 0.0294	0.9843 ± 0.0203
16–18*	55.8	2.7684 ± 0.0631	2.6757 ± 0.0615	2.3938 ± 0.0684	2.5038 ± 0.0710	0.8947 ± 0.0328	0.9665 ± 0.0220
18–20*	69.3	2.5761 ± 0.0527	2.6492 ± 0.0539	2.2782 ± 0.0754	2.3704 ± 0.0780	0.8600 ± 0.0334	1.0284 ± 0.0192
20–22	73.7	2.4614 ± 0.0465	2.4308 ± 0.0461	2.0032 ± 0.0607	2.0439 ± 0.0617	0.8241 ± 0.0294	0.9876 ± 0.0163
22–24*	72.3	2.6028 ± 0.0682	2.4694 ± 0.0656	2.1405 ± 0.0732	2.0249 ± 0.0699	0.8668 ± 0.0375	0.9488 ± 0.0243
24–26	47.5	4.5552 ± 0.1136	4.5768 ± 0.1141	3.7940 ± 0.1425	3.7414 ± 0.1407	0.8290 ± 0.0374	1.0047 ± 0.0229
26–28	28.1	5.8552 ± 0.1398	5.8680 ± 0.1398	4.5819 ± 0.1435	3.9500 ± 0.1281	0.7808 ± 0.0307	1.0022 ± 0.0238

* Samples are excluded from the calculation of the isochronous age for each of the corresponding depth intervals (explanations are given in the text).

Pollen zone 1 (260–254 cm): *Pinus* is the dominant pollen in the spectra (up to 67%). A high concentration of *Picea* pollen (up to 21%) is recorded. Herbaceous pollen is represented mainly by Cyperaceae and Poaceae. Among sporophytes, spores of the family Polypodiaceae are dominant.

Pollen zone 2 (254–238 cm). *Pinus* pollen (35–80%) and *Betula* sect. *Albae* (14–33%) dominate. Picea pollen decreases in abundance. The content of *Betula nana* pollen varies from 4 to 10%. Pollen grains of broadleaved species are present sporadically. The count of Polypodiaceae spores sharply increases (up to 41%).

Pollen zone 3 (238–220 cm). *Pinus* and *Betula* sect. *Albae* pollens are still dominant in the spectra. The amount of pollen of broadleaved tree species *Ulmus* and *Quercus* reaches 8%.

Pollen zone 4 (220–175 cm). The spectra are dominated by *Alnus* and *Corylus* pollen. A distinctive feature of this zone is the high content of *Quercus* (up to 34%) and *Ulmus* (up to 18%) pollen. The number of spores of the family Polypodiaceae decreases significantly.

Pollen zone 5 (175–60 cm). This zone is characterized by the absolute maximum of *Corylus* (33–45%) and *Alnus* (26–49%) pollen. The appearance of *Tilia* pollen (1–6%) is noted in the spectra of this zone. The count of *Quercus* pollen decreases to 5%. Spores of *Osmunda cinnamomea* are encountered for the first time.

Pollen zone 6 (60–4 cm). A special feature of this zone is the increasing amount of *Carpinus* pollen (up to 31%) in the spectra. *Osmunda cinnamomea* spores are present.

Table 2. ^{230}Th/U isochronous age of organogenic deposits in the studied sections from Tver and Smolensk Provinces

Depth, cm	Linear technique		Nonlinear technique		^{230}Th/U isochronous age*, ka,	Pollen zone (Grichuk, 1989)
	Age, ka	Confidence interval, ka	Age, ka	Confidence interval, ka		
			Granichnaya			
28–12 (5 samples)	101.9 ± 11/8.5 (R = 0.9842)	112–93	104.3 ± 3.6	108–101	108–101	M6 (main part)
			Kileshino			
570–545 (11 samples)	114.1 ± 2.7/2.4 (R = 0.9998)	117–112	114.7 ± 4.2	119–111	117–112	M4
			Bolshaya Dubenka			
90–74 (6 samples)	111.7 ± 10/8 (R = 0.983)	122–104	110.2 ± 5.3	116–105	116–105	M4
102–90 (6 samples)	113.9 ± 4.6/4.1 (R = 0.9982)	118–110	116.1 ± 4.1	120–112	118–112	M3
108–102 (4 samples)	114.9 ± 11.7/9.5 (R = 0.9928)	127–105	124.5 ± 11.3	136–113	127–113	M2
			Malaya Kosha			
180–96 (9 samples)	111.9 ± 6.6/5.3 (R = 0.988)	118–107	106.2 ± 5.9	112–100	112–107	M5
			Nizhnyaya Boyarshchina (Maksimov et al., 2022)			
137–119 (7 samples)	100.6 ± 4.6/4.1 (R = 0.9923)	105–97	96.5 ± 5.3	102–91	102–97	M6
179–165 (7 samples)	107.3 ± 3.0/2.7 (R = 0.9999)	110–105	109.8 ± 2.2	112–108	110–108	M5 (central part)
303–289 (7 samples)	127.6 ± 3.7/3.3 (R = 0.9996)	131–124	128.1 ± 2.0	130–126	130–126	M1 (upper part)

R is the coefficient of linear correlation;* interval of overlapping confidence intervals by linear and nonlinear techniques.

Pollen zone 7 (4–0 cm). Pollen from *Betula* sect. *Albae, Betula nana, Salix, Alnus, Quercus, Carpinus, Cyperaceae*, and *Poaceae* is detected. Occasional spores of Polypodiaceae and *Sphagnum* are recorded. The content of pre-Quaternary spores and pollen in this zone reaches 25%.

The comparison of our data with the results of the previous studies of the deposits on the Malaya Kosha River [7, 8] revealed similarities in the obtained pollen and spore spectra with the stages of the development of vegetation during the Mikulino Interglacial (M1–M7 zones).

The accumulation of clays (260–238 cm) in this area was accompanied by the spread of sparse spruce forests (pollen zone 1) and later birch and pine forests (pollen zone 2). According to the biostratigraphic scheme proposed by V.P. Grichuk [5], these pollen zones correspond to zones M1 and M2 of the Mikulino Interglacial. Later on (pollen zone 3), the role of pine–birch forests with the presence of oak and elm trees increased, which is comparable to zone M3. At the same time, lacustrine sedimentation began. The further expansion of oak forests with the participation of elm, hornbeam, alder, and hazel corresponds to zone M4. The next stage of vegetation development is characterized by the distribution of polydominant broadleaved forests consisting of oak, elm, hornbeam, and linden trees with hazel and alder in the shrub layer (zone M5). Osmunda fern grew in the herbaceous layer. At the following stage (M6 zone), the role of hornbeam in broadleaved forests increased with the participation of hazel and alder.

Paleocarpological analysis. The species composition of carpological remains and their quantity in 17 samples are shown in the carpological diagram (Fig. 7). Two LCCs are identified in the section studied.

In the LCC of MK-1 (depth of 130–200 cm), the dominant remains of semi-aquatic plants are represented by numerous nutlets of *Schoenoplectus lacustris* and a *Carex* sp. *Cladium mariscus* nutlet is also identified. Remains of aquatic plants include seeds of *Najas marina* and *Caulinia flexilis*, endocarps of pondweeds, and fragments of water lily seeds (*Nuphar* sp.). The remains of woody species are mainly alder nutlets. Furthermore, remains of broadleaved species, such as

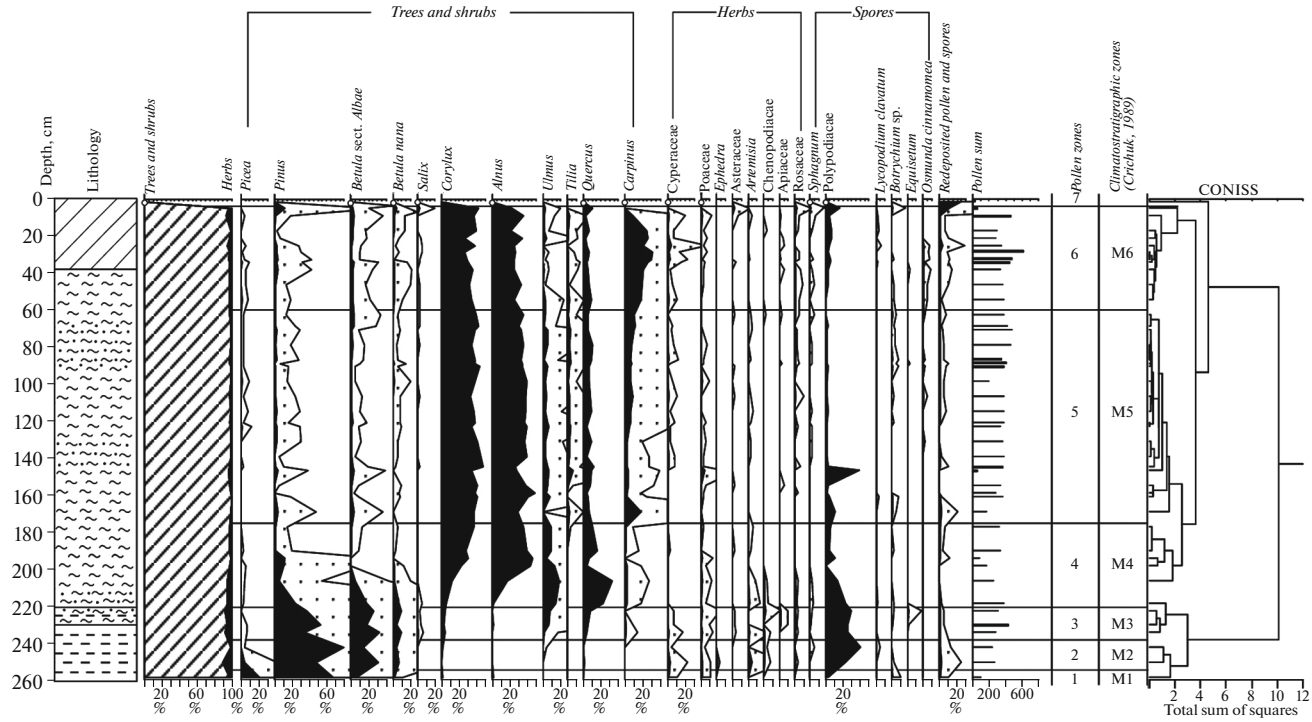

Fig. 6. Spore–pollen diagram for the deposits of the Malaya Kosha section.

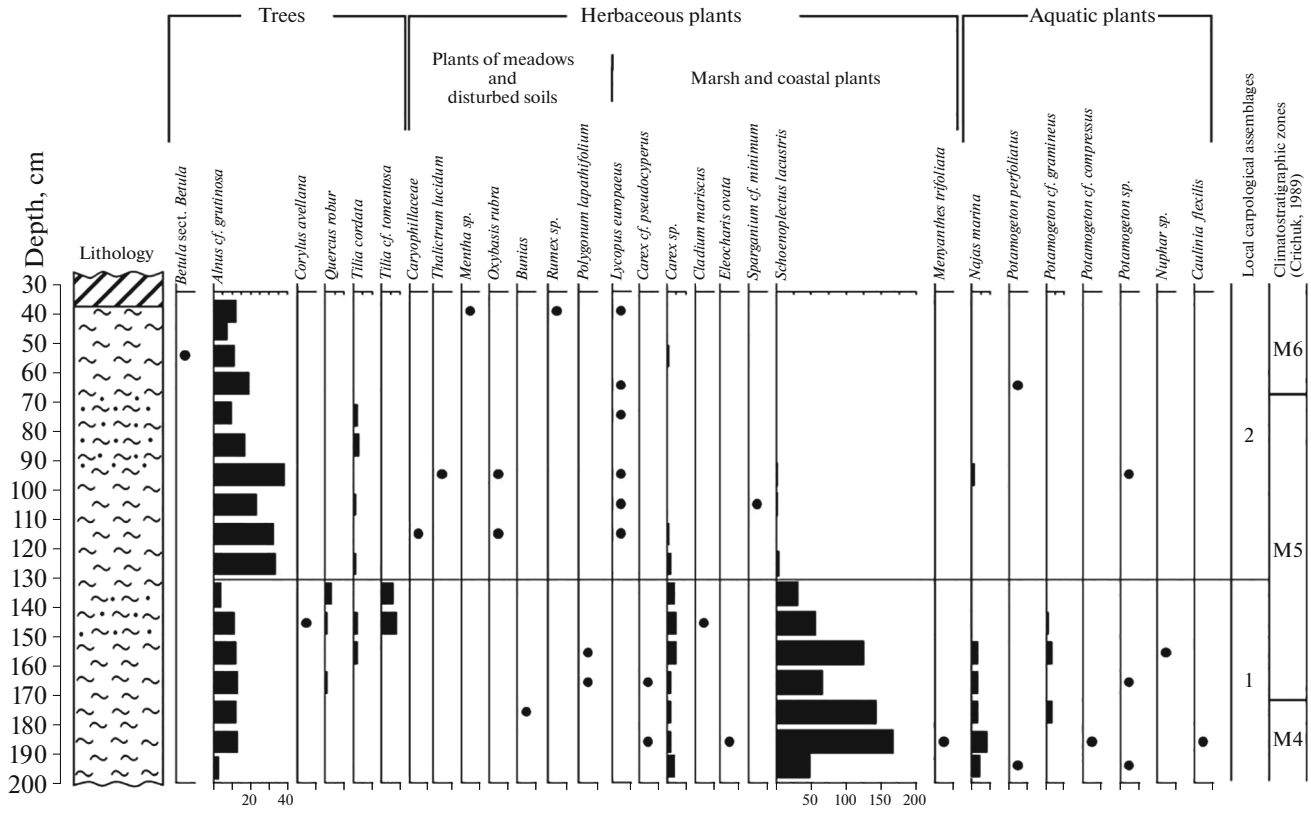

Fig. 7. Carpological diagram of the deposits from Malaya Kosha section. The horizontal axes show the number of remains in a sample; 1, single carpological remains (<5); designations on the lithological core are given in Fig. 2.

acorn cups (*Quercus robur*) and fruits of the linden tree (*Tilia tomentosa* and *Tilia* sp.) are identified. Fragments of hazel nut shells (*Corylus avellana*) are found among shrub plant remains. Remains of plants from disturbed substrates are represented by sporadic fruits of *Bunias* cf. *orientalis* and *Polygonum lapathifolium*.

The LCC of MK-2 (depth of 35–130 cm) is characterized by a sharp decrease in the number of *Schoenoplectus lacustris* fruits and an increase in the number of alder nutlets. The remains of broadleaved tree species are represented by scarce linden fruits. Not all samples were found to contain remains of aquatic plants in small quantities. The presence of plant remains from important habitats (*Lycopus europaeus*, *Thalictrum lucidum*) and disturbed soils (*Oxybasis rubra*, *Rumex* sp.) increases. Faunal remains also occur in this interval; a fish vertebra was found in the sample from a depth of 80–90 cm, and bryozoan statoblasts were discovered in the sample from a depth of 60–70 cm.

The identified carpological complexes are similar in composition to the complex distinguished previously at the same location, where *Tilia tomentosa* fruits were also identified [8].

Both LCCs contain species of coastal and aquatic plants, which are also typical of the flora during the Mikulino Interglacial: *Cladium mariscus, Najas marina*, and *Caulinia flexilis*. This allows us to associate the studied flora with the most heat-provided phases of the Mikulino Interglacial. The comparison with the palynological data showed that the LCC of MK-1 corresponds to the end of the M4 "oak and elm" pollen zone and the first half of the M5 "linden" zone. The LCC of MK-2 matches the second half of the M5 zone and the beginning of the M6 "hornbeam" zone, i.e., the climatic optimum of the Mikulino Interglacial.

^{230}Th/U dating. The values of the ^{228}Th/^{232}Th activity ratio in the samples along the vertical profile of organic-rich deposits in the upper layers within the depth range of 38–90 cm deviated from unity by more than $\pm 1\sigma$. The conditions of a closed radiometric system were likely disturbed in this segment over the past 25–30 years.

Consequently, detailed radiochemical analysis of the U and Th isotopes was conducted for the samples collected from the depth range of 96–180 cm (Table 1), matching the M5 pollen zone. Several samples at a depth of 168–172 cm are likely associated with explicitly open radiometric systems. The ^{234}U/^{238}U activity ratios in these samples are much lower than unity (i.e., by more than 1σ), which results from mostly post-sedimentation leaching of ^{234}U from the deposits in accordance with the Cherdyntsev–Chalov effect [19]. Without these samples, the confidence intervals of isochronous age, calculated using both linear ($122 \pm 7/5$ ka) and nonlinear (104 ± 8 ka) methods for a series of 14 samples, do not overlap due to insufficiently high correlation coefficients of the linear relationships in the respective coordinates. By excluding several more samples (Table 1), we estimate the isochronous age with overlapping time intervals using both methods (Table 2). Thus, the sequence at the depths of 96–180 cm, corresponding to most of the M5 zone, was deposited approximately in the interval of ~112–107 ka.

Granichnaya Section

Pollen analysis. Four pollen zones were identified (Fig. 8).

Pollen zone 1 (82.5–60 cm): The spectra are dominated by herbaceous pollen (30–65%). Pollen from woody and shrub species, such as *Pinus*, *Betula* sect. *Albae*, *Betula nana*, *Picea*, and *Salix*, occurs in small amounts. The count of pre-Quaternary pollen and spores was 7%.

Pollen zone 2 (60–30 cm): The first half of this zone (2a) is characterized by the increasing count of tree and shrub pollen, mainly due to *Picea* and *Pinus*. The pollen of *Artemisia* and *Cyperaceae* dominates in the group of grass plants; *Ephedra* pollen is also identified. In the second half of the zone (2c), *Picea* pollen reached its peak (36%) and *Alnus* (17–27%) and *Corylus* (7–13%) pollen appeared. Sporophytes are dominated by *Polypodiaceae* spores.

Pollen zone 3 (30–2 cm). The spore–pollen spectra differ sharply from the previous zone in abundant pollen of *Alnus* (37–60%), *Corylus* (13–26%), and broadleaved species. The curve of the *Carpinus* pollen content reaches a peak of 16%; *Quercus*, 6%; while *Tilia* and *Ulmus*, make up 2% each. The count of herbaceous pollen does not exceed 6%. Sporophytes are dominated by *Sphagnum* and *Polypodiaceae* spores; spores of *Osmunda cinnamomea* occur constantly.

Pollen zone 4 (2.5–0 cm). Sporadic pollen grains of *B. nana*, *Alnus*, and spores of *Sphagnum*, *Polypodiaceae*, and *Lycopodium clavatum* are found in the pollen and spore spectra.

We compared the identified palynozones with the zones proposed by V.P. Grichuk [5] for the Mikulino Interglacial. Pollen zone 2 matches the beginning of the Mikulino Interglacial and corresponds to zone M1. This is the time when isolated spruce and pine forests with elements of periglacial flora (*Betula nana*, *Salix*, and *Ephedra*) developed. The sharp boundary between clay and peat at a depth of 30 cm is likely to mark a nondepositional hiatus. Pollen zone 3 corresponds to zone M6 and matches the end of the climatic optimum of the Mikulino Interglacial. In the surrounding territory, polydominant broadleaved forests grew with dominant hornbeam, the participation of alder, and an abundant shrub layer of hazel; Osmunda was present in the herbaceous layer. Zones M2–M5, as well as M7 and M8, were not found in this section. Thus, the Granichnaya section represents the

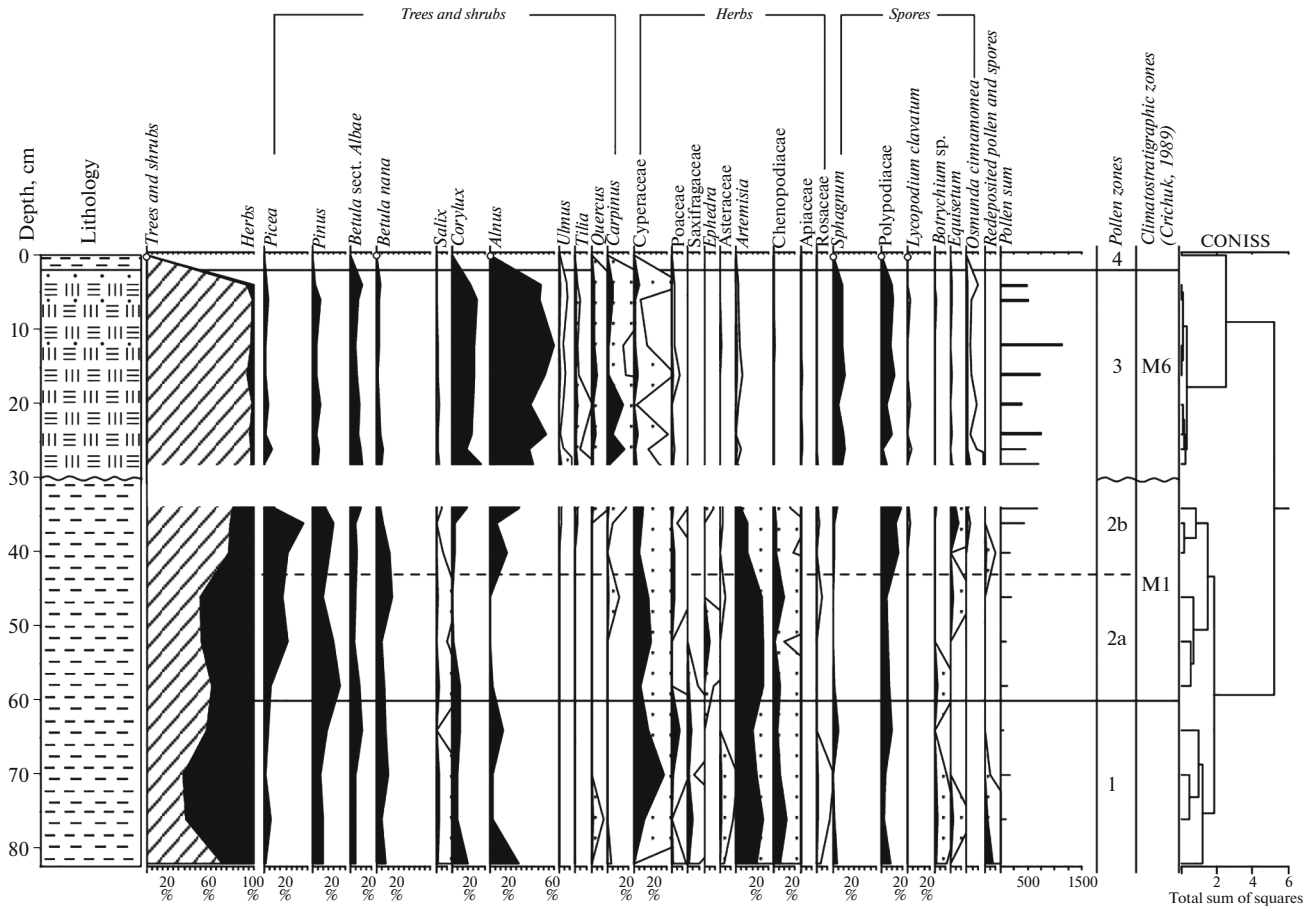

Fig. 8. Spore–pollen diagram of the sediments from the Granichnaya section.

deposits that were formed in the initial phase (M1 zone) and in the second half of the Mikulino Interglacial (M6 zone).

^{230}Th/U dating. The peat stratum from a depth of 2–30 cm was heavily waterlogged, which could affect the preservation of a closed radiometric system in the deposits. The experimental work revealed the following circumstances. On the one hand, the value of ^{228}Th/^{232}Th activity ratios along the vertical profile of the peat varied around unity within the error, indicating the maintenance of conditions for a closed radiometric system in the deposits over the last 25–30 years. On the other hand, the main analytical data (Table 1) showed that, in some layers, these conditions were disturbed much earlier. The upper sample of the peat underwent post-sedimentation accumulation of U, which resulted in an evidently low value of the ^{230}Th/^{234}U activity ratio. The use of this sample in isochronous calculations leads to a significant rejuvenation. In four samples from the depths of 4–10 cm, 16–18 cm, and 22–24 cm, the values of the ^{234}U/^{238}U activity ratios are significantly less than unity, by more than 1σ. These layers showed predominant post-sedimentation leaching of ^{234}U by the Cherdyntsev–Chalov effect [19]. For a set of five samples that are most suitable for constructing linear dependences in the depth range of 12–28 cm (Table 1), we obtained an age of 108–101 ka, corresponding to zone M6 (Table 2). We note that under the conditions of highly waterlogged sediments, this estimate is quite approximate.

Kileshino-2 Section

Paleobotanical studies of the section showed that the lower part of the deposits on the interval of 5.4–8.9 m was formed during the first half of the Mikulino Interglacial [13]. Only the upper portion of this section (5.40–5.70 m) consisted of organogenic deposits, attributed to pollen zone M4, which could be suitable for ^{230}Th/U dating.

^{230}Th/U dating. We studied the samples of the loamy-peat stratum collected at the depth of 5.45–5.70 m relative to the vertical profile (Table 1). It is quite challenging to assess the preservation of a closed radiometric system in the post-sedimentation period in such a narrow segment. However, the fulfillment of this premise is evidenced by both the values of the ^{228}Th/^{232}Th activity ratios in the samples, which were

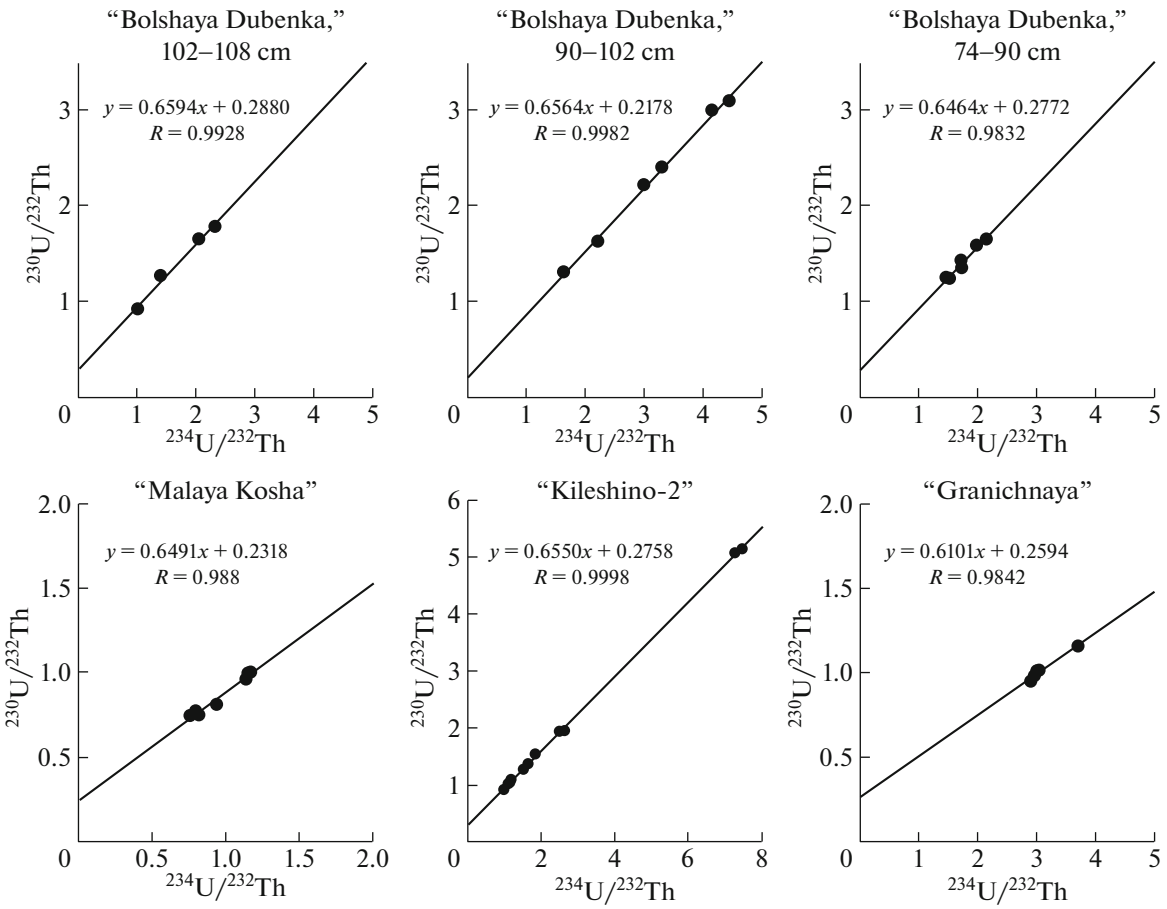

Fig. 9. Linear dependences according to the analytical data of the studied sections in the coordinates $^{230}Th/^{232}Th–^{234}U/^{232}Th$.

equal to unity within the error, and the linear dependences with high correlation coefficients and a wide spread of dots relative to each other constructed for all samples (Fig. 9). In two samples, the values of the $^{234}U/^{238}U$ activity ratios are slightly less than unity, but with regard to the error, they are greater than unity (Table 1) and their removal from the linear regression has little impact on the value of the isochronous age.

Therefore, to determine the isochronous age, we used the analytical data of all 11 samples (Table 1) and established (Table 2) that sedimentation in the Kileshino-2 section, corresponding to pollen zone M4 [13], presumably occurred 117–112 ka.

DISCUSSION

The results of paleobotanical studies in three sections in Tver Province presented in this work along with the published data (Kileshino-2 section [13] and Nizhnyaya Boyarshchina section [4]) made it possible to reveal the main stages in the development of vegetation during the Mikulino Interglacial and to compare them with the scheme by V.P. Grichuk [5] (Table 3). The age of individual development phases of vegetation was estimated by $^{230}Th/U$ dating (Table 2). The obtained intervals fit into the time frames of the published age estimates for the Mikulino deposits in the Nizhnyaya Boyarshchina section [4] and do not contradict the results of $^{230}Th/U$ dating for several Mikulino and Eemian organic-rich deposits studied at different times [3, 6, 14].

The reliability of $^{230}Th/U$ age estimates depends primarily on the degree of fulfillment of the premises for the $^{230}Th/U$ isochronous approximation, which is quite difficult to assess in a strict sense. From this perspective, the samples used for isochronous constructions should not exhibit clear signs of an open radiometric system. The dates estimated from the parameters of linear dependences with high correlation coefficients and a significant spread of analytical dots are more substantiated. They should be at least 4–5 in a series. Relatively reliable isochronous structures and, consequently, age estimates were obtained for the deposits in the Kileshino-2 section, 117–112 ka, and Bolshaya Dubenka section (90–102 cm), 118–112 ka. The analytical data from these sections presented in the $^{230}Th/^{232}Th–^{234}U/^{232}Th$ coordinates (which are fundamental for age estimation) conform better

Table 3. Correlation of paleobotanical data for the sections in Tver and Smolensk provinces and a possible chronological scheme for the Mikulino Interglacial

Palynozones					Zones by V.P. Grichuk (1989)	^{230}Th/U age, ka	Suggested chronological scheme, ka
Nizhnyaya Boyarshchina[1]	B. Dubenka[2]	Malaya Kosha[3]	Kileshino-2[4] (Karpukhina et al., 2022)	Granichnaya[5]			
Zone of spruce (upper maximum of spruce), pine and birch with participation of elm, alder, and hazel	Zone of spruce (upper maximum of spruce), pine, alder, hazel, and hornbeam	–	–	–	M7		~100
Zone of spruce and pine with participation of birch, alder, hazel, hornbeam (maximum of hornbeam), linden; Osmunda is present	Zone of spruce with participation of hornbeam (maximum of hornbeam) alder, hazel, and linden; Osmunda is present	Zone of hazel, alder, and hornbeam (maximum of hornbeam) with participation of oak, linden, and hornbeam; Osmunda is present	–	Zone of alder, hazel, and hornbeam (maximum of hornbeam) with participation of oak, linden, and hornbeam; Osmunda is present	M6	102–97[1] 108–101[5]	
Zone of hazel and alder (maximum of hazel and alder) with participation of oak and elm; hornbeam and linden appear	Zone of hazel and alder (maximum of hazel and alder) with participation of oak and elm; hornbeam and linden appear	Zone of hazel and alder (maximum of hazel and alder) with participation of oak, elm, hornbeam, and linden; Osmunda is present	–	–	M5	112–107[3] 110–108[1]	
Zone of oak (maximum of oak) with participation of elm; hazel and alder appear	Zone of oak and elm (maximum of oak and elm); hazel appears	Zone of oak and elm (maximum of oak and elm), hazel and alder; hornbeam is present	Zone of hazel and alder, pine, with participation of oak and elm (maximum of elm); Brasenia is present	–	M4	116–105[2] 117–112[4]	~112
Zone of pine and birch with participation of oak, elm							

Table 3. (Contd.)

Palynozones					Zones by V.P. Grichuk (1989)	^{230}Th/U age, ka	Suggested chronological scheme, ka
Zone of pine and birch; elm appears	Zone of birch and pine; elm appears	Zone of pine and birch; elm, oak, hornbeam, hazel appears	Zone of pine, oak (maximum of oak) and elm; Osmunda is present	–	M3	118–112[2]	
Zone of pine and birch; with participation of spruce, ephedra is present	Zone of pine with participation of birch, ephedra is present	Zone of pine and birch; ephedra is present			M2	127–113[2]	~118
Zone of spruce (lower maximum of spruce) with low participation of pine and birch; relatively high participation of grasses, ephedra is present	Zone of spruce (lower maximum of spruce) with participation of pine and birch	Zone of spruce (lower maximum of spruce) and pine with participation of birch	Zone of spruce (lower maximum of spruce) with participation of pine and birch; relatively high participation of grasses, ephedra is present	Zone of spruce (lower maximum of spruce) with low participation of pine and birch; relatively high participation of grasses, ephedra is present	M1	130–126[1]	~126 ~130

[1, 2, 3, 4, 5] Correspondence of ^{230}Th/U age to a particular section.

to the above conditions than in the other cases of dating (Fig. 9).

According to the data of studying the deposits in the Nizhnyaya Boyarshchina section, we made a conclusion about the relative reliability of the ^{230}Th/U age estimates, 130–126 ka for the upper half of M1 and 110–108 ka for the central part of M5 [4]. Thus, the age reconstruction of the Last Interglacial can rely on these four reference dates, which do not contradict the confidence intervals of other age estimates that probably are less reliable. Therefore, we consider a possible variant of chronology for the Mikulino Interglacial (Table 3).

Its lower boundary, corresponding to the second half of the M1 zone [1, 5], is estimated at 130–126 ka according to the dates of the gyttja layers in the Nizhnyaya Boyarshchina section, which were formed in the second half of zone M1 [4]. This estimate is in good agreement with the onset of marine isotope substage MIS-5e [20]. The M1 transition zone from the Moscow Glaciation is reflected in all studied sections and shows the dominance of sparse pine, birch, and spruce forests with periglacial flora (dwarf birch, willow, wormwood, ephedra, etc.).

In the subsequent phase (M2), the proportion of pure spruce cenoses decreases, and pine becomes the dominant tree species with the participation of birch. This stage of vegetation development began ~126 ka and ended ~118 ka. Later on, elm appeared in the pine–birch forests almost simultaneously across the study region. In addition, oak, hazel, and hornbeam occurred in the Malaya Kosha section and only oak was present in the Kileshino-2 section. Such changes in the vegetation composition were recorded in zone M3. In the Nizhnyaya Boyarshchina section, oak had already existed in zone M4, while hazel and alder began to spread across the entire territory. These events (M3–M4) occurred in the interval of ~118–112 ka.

The widespread occurrence of thermophilic flora (oak, elm, hornbeam, linden, and hazel) began ~112 ka (M5 zone) and ended ~100 ka. Hornbeam showed the peak expansion (M6 zone) in the same age interval in all sections studied. The final stage of the Mikulino Interglacial (M7 zone) was only recorded in the Nizhnyaya Boyarshchina and Bolshaya Dubenka sections. Around 100 ka, the participation of coniferous species in mixed coniferous–broadleaved forests began to increase, mainly due to spruce. Alder and

hazel became widely distributed; hornbeam remained the dominant broadleaved tree species.

Thus, we assume that the Mikulino Interglacial from the beginning of zone M2 to the end of M6 lasted approximately from 126 to 100 ka. Taking into account that its final phases M7–M8 were not dated, the entire interglacial might have been no shorter than 25 000 years. We note that the formation of zone M1 began earlier than 130 ka. Therefore, the time interval of zones M1–M8 should be even longer.

The estimate of the Mikulino Interglacial period obtained based on the results of this work goes beyond the time limits of MIS-5e and differs from the data of a few other studies ([1, 2] and others). This is mainly caused by significant differences in the dates of the final phases in this period. The reason for the discrepancies is likely related to the use of different indicators (oxygen isotopes, pollen and spores, diatoms, etc.) in marine and continental sediments, which indicate the end of the interglacial period, as well as to the application of different geochronometrical methods.

In general, we note a small number of dates that could directly fix the time limits for the Mikulino Interglacial phases. From this perspective, the chronological scheme presented in this work has a probabilistic nature and requires further substantiation, including statistical confirmation and further refining.

CONCLUSIONS

The deposits from the four sections in Tver Province studied in this work are correlated with the pollen zones of the Mikulino Interglacial (M1–M7) (Table 3). The ^{230}Th/U age covers the zones from the beginning of M2 to the end of M6 within the range of 127–101 ka. In the Nizhnyaya Boyarshchina section, the age interval of 130–97 ka is calculated from the middle of zone M1 to the end of zone M6 [4]. The following conclusions can be drawn from this work.

(1) The detailed paleobotanical studies confirmed that the examined deposits from the four sections in Tver Province belong to the Mikulino Interglacial. The biostratigraphic zoning of the sections was performed, which made it possible to correlate the deposits with the pollen zones of the stratigraphic scheme by V.P. Grichuk [5].

(2) The uniform composition of the vegetation characterized by sparse pine, birch, and spruce forests with the participation of periglacial flora is typical across the entire territory from approximately 130 ka (and perhaps earlier) up to ~126 ka.

(3) The synchronous appearance of elm on the study territory, gradual spread, and maximum participation of other broadleaved species occurred after ~118 ka.

(4) According to the ^{230}Th/U dates and the data of the paleobotanical analysis of the organic-rich deposits from the four sections in Tver Province and the Nizhnyaya Boyarshchina section in Smolensk Province, a simplified chronological scheme was proposed for the major stages of vegetation during the Mikulino Interglacial. It began ~130–126 ka (perhaps somewhat earlier). Its first phase, corresponding to zone M2, ended ~118 ka. The pre-optimal stages of vegetation development (M3 and M4 zones) fall within the time interval of ~118–112 ka. The climatic optimum of the interglacial (M5 and M6 zones) started ~112 ka and ended ~100 ka.

(5) The duration of the Mikulino Interglacial was likely to have been at least 25000 years.

FUNDING

This study was supported by the Russian Foundation for Basic Research, project no. 20-05-00813 (fieldwork, ^{230}Th/U dating, spore–pollen analysis, processing and interpretation of paleobotanical data) and under a State Assignment of the Botanical Institute, Russian Academy of Sciences, project no. 122011900029-7 (carpological analysis). The paleocarpological data were processed within the framework of a State Assignment of the Institute of Geography, Russian Academy of Sciences, project no. AAAA-A19-119021990091-4 (FMGE-2019-0005).

CONFLICT OF INTEREST

The authors of this work declare that they have no conflicts of interest.

REFERENCES

1. E. Yu. Novenko, *Changes in Vegetation and Climate of the Central and Eastern Europe in the Late Pleistocene and Holocene at the Interglacial and Transitional Stages of Climatic Macrocycles* (GEOS, Moscow, 2016) [in Russian].
2. N. S. Bolikhovskaya and A. N. Molod'kov, in *Proc. All-Russian Conf. with International Participation "The 2020 Markov Readings" Actual Problems of Pleistocene–Holocene Paleogeography* (Faculty of Geography MSU, Moscow, 2020), pp. 63–70 [in Russian].
3. F. E. Maksimov, V. Yu. Kuznetsov, L. A. Savel'eva, V. A. Grigor'ev, A. Yu. Petrov, A. P. Fomenko, and N. G. Baranova, in *Proc. 2nd All-Russian Sci. Conf. Ways of Evolution Geography* (Inst. Geogr. Russ. Acad. Sci, Moscow, 2021), Iss. 2, pp. 812–816 [in Russian].
4. F. E. Maksimov, L. A. Savel'eva, S. S. Popova, I. S. Zyuganova, V. A. Grigor'ev, S. B. Levchenko, A. Yu. Petrov, A. P. Fomenko, L. A. Pankratova, and V. Yu. Kuznetsov, Izv. Ross. Akad. Nauk, Ser. Geogr. **86** (3), 447–469 (2022). https://doi.org/10.31857/S2587556622030116
5. V. P. Grichuk, *The History of Flora and Vegetation* (Nauka, Moscow, 1989) [in Russian].
6. F. E. Maksimov and V. Yu. Kuznetsov, Vestn. S.-Peterb. Univ., Ser. 7, No. 4, 94–107 (2010).

7. N. S. Chebotareva, M. A. Nedoshivina, and T. I. Stolyarova, Byull. Kom. Chetvertichn. Perioda, No. 26, 35–49 (1961).
8. E. N. Ananova, E. P. Zarrina, T. I. Kazartseva, and I. I. Krasnov, Byull. Kom. Chetvertichn. Perioda, No. 40, 22–34 (1973).
9. L. T. Semenenko and V. B. Kozlov, Byull. Kom. Chetvertichn. Perioda, No. 42, 154–158 (1974).
10. I. V. Kotlukova, in *Boundary Formations of Continental Glaciations* (Nauka, Moscow, 1972), pp. 225–232 [in Russian].
11. R. E. Giterman, N. P. Kuprina, and E. V. Shantser, Byull. Kom. Chetvertichn. Perioda, No. 44, 84–88 (1975).
12. K. Lasberg, V. Kalm, and K. Kihno, Est. J. Earth Sci. **63** (2), 88–96 (2014). https://doi.org/10.3176/earth.2014.08.
13. N. V. Karpukhina, V. V. Pisareva, I. S. Zyuganova, E. A. Konstantinov, A. L. Zakharov, D. V. Baranov, A. O. Utkina, and A. V. Panin, Izv. Ross. Akad. Nauk, Ser. Geogr. **84** (6), 874–887 (2020). https://doi.org/10.31857/S2587556620060060
14. M. A. Geyh, Geochronometria **20**, 9–14 (2001).
15. A. Böerner, A. Hrynowiecka, V. Kuznetsov, R. Stachowicz-Rybka, F. Maksimov, V. Grigoriev, M. Niska, and M. Moskal-del Hoyo, Quat. Int. **386**, 122–136 (2015). https://doi.org/10.1016/j.quaint.2014.10.022
16. V. P. Grichuk and E. D. Zaklinskaya, *Analysis of Fossil Pollen and Spores and Its Application in Paleogeography* (Geografgiz, Moscow, 1948) [in Russian].
17. P. D. Moore, J. A. Webb, and M. E. Collinson, *Pollen Analysis* (Oxford, 1991).
18. V. P. Nikitin, *Paleocarpological Method* (Tomsk State Univ., Tomsk, 1969) [in Russian].
19. V. V. Cherdyntsev and P. I. ChalovUSSR Inventor's Certificate No. 163 (Central Sci. Res. Design Inst., Moscow, 1977).
20. T. Litt and P. Gibbard, Episodes **31** (2), 260–263 (2008). https://doi.org/10.18814/epiiugs/2008/v31i2/015

Translated by L. Mukhortova